Open access • Journal Article • DOI:10.1190/1.1543192

Fluid-property discrimination with AVO: A Biot-Gassmann perspective

Brian Russell, Ken Hedlin, Fred Hilterman, Larry Lines

Institutions: Husky Energy, University of Calgary

Published on: 01 Jan 2003 - Geophysics (Society of Exploration Geophysicists)

Fluid-property discrimination with AVO: A Biot-Gassmann perspective

Brian H. Russell, Ken Hedlin[1], Fred J. Hilterman[2], and Laurence R. Lines

ABSTRACT

This paper draws together basic rock physics, AVO, and seismic amplitude inversion to discuss how fluid discrimination can be performed using pre-stack seismic data. From both Biot and Gassmann theories for porous, fluid-saturated rocks, a general formula is first derived for fluid-property discrimination given that both the P and S impedances are available. In essence, an AVO inversion is transformed into the elastic properties of the pore space. This formula provides a more sensitive discriminator of the pore-fluid saturant than the acoustic impedance and is especially applicable in hard-rock environments. The formulation can be expressed with either the Lamé constants and density, or the bulk and shear moduli and density. Numerical and well-log examples illustrate the applicability of this approach. The combination of an AVO inversion and the parameters of the formula are then discussed to show how this technique can be implemented using pre-stack seismic data. Finally, a shallow gas-sand example from Alberta and a well-log example from Eastern Canada are shown to illustrate the techniques.

INTRODUCTION

Recently, there has been a lot of interest in the extraction of information about the fluid content of the reservoir using Amplitude Variations with Offset Analysis, or AVO. Goodway et al (1997) proposed the lambda-mu-rho technique, which has met with much success. Hedlin (2000) proposed the pore-modulus method, which was based on work by Murphy et al (1993). Most recently, Hilterman (2001 SEG Distinguished Instructor Short Course) introduced the concept of the fluid discriminant.

In this paper we will examine all of these concepts in the context of the Biot-Gassmann theory. This will involve looking at the differences in formulation between the Biot and Gassmann theories of porous media (Kreif et al, 1990). By doing this, it will become obvious that the important distinction that we need to make when extracting fluid-property information is between the dry and saturated components of the reservoir, and not the constants used to describe the reservoir (i.e. Lamé constants versus bulk and shear moduli). We can then relate the various dry rock elastic constant ratios to the techniques summarized above, and provide a physical framework that ties together these apparently disparate methods.

[1] Husky Energy Ltd, 707 – 8th Avenue SW, Calgary, Alberta, Canada T2P 3G7

[2] Geophysical Development Corporation, 8401 Westheimer, Suite 150, Houston, Texas, USA 77063-2799

BIOT-GASSMANN THEORY OF VELOCITY IN POROUS ROCKS

The basic equations for P and S-wave velocity in isotropic, non-porous media are well known and can be written as

$$V_P = \sqrt{\frac{\lambda + 2\mu}{\rho}} = \sqrt{\frac{K + \frac{4}{3}\mu}{\rho}}, \tag{1}$$

$$V_s = \sqrt{\frac{\mu}{\rho}}, \tag{2}$$

where ρ is the density, λ is the 1st Lamé parameter, μ is the 2nd Lamé parameter or shear modulus, and K is the bulk modulus, or the inverse of compressibility. Since the P-wave velocity in equation (1) has been written in two separate ways, it is obvious that the relationship between K and λ, which can be written as

$$K - \lambda = \tfrac{2}{3}\mu, \tag{3}$$

is exact. When we turn our attention to porous, saturated rocks, the situation becomes more complicated. The problem was first addressed by Biot (1941) and then Gassmann (1951) using apparently different approaches but, as shown by Krief et al (1990), these two approaches lead to the same results. Although there have been many theories proposed since Biot and Gassmann, their method has remained the most robust and frequently implemented way of expressing the P- and S-wave velocities of porous rocks in terms of elastic constants.

To understand the Biot-Gassmann terminology, we refer to Figure 1, which shows that a cube of porous rock can be characterized by four components: the rock mineral, the pore/fluid system, the dry-rock frame, or skeleton, and the saturated rock itself.

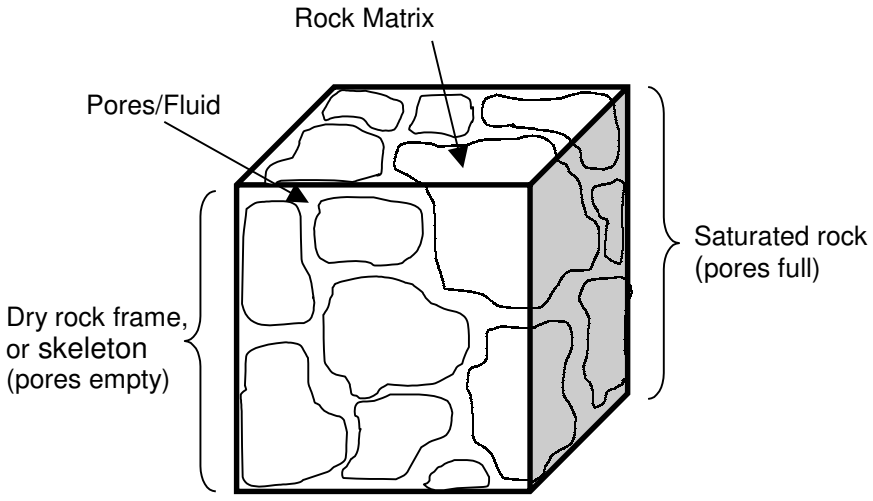

FIG. 1. In Biot-Gassmann theory, a cube of rock is characterized by four components: the rock matrix, the pore/fluid system, the dry rock frame, and the saturated frame.

The density effects of the saturated rock can be computed quite accurately with the volume average equation as

$$\rho_{sat} = \rho_m(1-\phi) + \rho_w S_w \phi + \rho_{hc}(1-S_w)\phi \quad , \tag{4}$$

where ρ_{sat} is the total density value, ρ_m is the density of the rock matrix, ρ_w is the density of water (brine), ρ_{hc} is the density of the hydrocarbons, ϕ is the porosity of the rock, and S_w is the water saturation.

A similar equation, which was an extension of Wyllie's empirical time-average equation, was proposed for velocity where transit-time, or inverse velocity, is substituted for density in equation (4), but this formulation was shown (Domenico, 1974) not to hold for gas sands. Domenico showed in the same paper that the Biot-Gassmann theory provides a much better fit for gas sands. Thus, we will now present a short review of this theory. However, instead of starting with Gassmann's work, as is usually done, we will start with the work of Biot (1941). Biot used the Lamé parameters and showed that (Krief et al, 1990)

$$\lambda_{sat} = \lambda_{dry} + \beta^2 M \quad , \tag{5}$$

where λ_{sat} is the 1st Lamé parameter for the saturated rock, λ_{dry} is the 1st Lamé parameter for the dry frame, β is the Biot coefficient, or the ratio of the volume change in the fluid to the volume change in the formation when hydraulic pressure is constant, and M is the modulus, or the pressure needed to force water into the formation without changing the volume. (Note that this modulus is different than the usual definition, in which the modulus represents the numerator under the square-root sign in the velocity equations.)

On the other hand, Gassmann started with the bulk and shear moduli, and derived the following relationship (Krief et al, 1990):

$$K_{sat} = K_{dry} + \beta^2 M \quad , \tag{6}$$

where K_{sat} is the bulk modulus of the saturated rock, K_{dry} is the bulk modulus of the dry rock, and β and M are the same as in equation (5). By equating equations (5) and (6), and using equation (3), the following result can be derived:

$$\mu_{sat} = \mu_{dry} \quad . \tag{7}$$

That is, the shear modulus is unaffected by the pore fluid. This theoretical result has a strong intuitive basis, since we know that fluids do not support shears, only compressions. Returning to equation (6), Gassmann further showed that

$$\beta = 1 - \frac{K_{dry}}{K_m} \quad , \tag{8}$$

and

$$\frac{1}{M} = \frac{\beta - \phi}{K_m} + \frac{\phi}{K_{fl}}, \tag{9}$$

where K_m is the bulk modulus of the matrix material and K_{fl} is the bulk modulus of the fluid. If equations (8) and (9) are substituted into equation (6) the result is the expression often seen in rock-physics textbooks (e.g. Mavko et al 1998). However, we have chosen to retain the use of the term $\beta^2 M$ for the difference between the dry and saturated cases to emphasize its independence from the first term. (Note that Murphy et al (1993) call this term K_P, or pore space modulus). Using $\beta^2 M$, we can rewrite the equation for P-wave velocity (equation 1) in the saturated case as

$$V_P = \sqrt{\frac{\lambda_{dry} + 2\mu + \beta^2 M}{\rho_{sat}}} = \sqrt{\frac{K_{dry} + \frac{4}{3}\mu + \beta^2 M}{\rho_{sat}}}, \tag{10}$$

or, more succinctly, as

$$V_P = \sqrt{\frac{s + f}{\rho_{sat}}}, \tag{11}$$

where f is a fluid/porosity term equal to $\beta^2 M$, and s is a dry-skeleton term which can be written either as $K_{dry} + \frac{4}{3}\mu$ or $\lambda_{dry} + 2\mu$. Note that in equations (10) and (11) we have assumed that $\mu = \mu_{sat} = \mu_{dry}$.

EXTRACTING THE FLUID TERM

Since we will be applying this method to seismic data, a practical limitation that will be discussed later is that we can estimate only the P and S-wave impedances, Z_P and Z_S, rather than velocities V_P and V_S, where

$$Z_P = \rho V_P = \sqrt{\rho(f + s)}, \tag{12}$$

and

$$Z_S = \rho V_S = \sqrt{\rho\mu}. \tag{13}$$

We will discuss the actual computation of the impedances in a later section. First, let's do a little more mathematics. To remove the square roots in the above equations, we need to square the impedances, to get

$$Z_P^2 = \rho(f + s), \tag{14}$$

and

$$Z_S^2 = \rho\mu \quad . \tag{15}$$

To extract the fluid component ρf, we therefore need to find a constant, c, which, when multiplied by Z_S^2 and subtracted from Z_P^2, will produce the desired result. Mathematically, this can be written as

$$\rho f = Z_P^2 - cZ_S^2 = \rho\left(f + s - c\mu\right) \quad . \tag{16}$$

In other words, we need to find a value of c such that the product of c and μ is equal to the dry skeleton term. By inspection from equation (10), this can be written in one of three ways:

$$c = \frac{\lambda_{dry}}{\mu} + 2 = \frac{K_{dry}}{\mu} + \frac{4}{3} = \left[\frac{V_P}{V_S}\right]_{dry}^2 . \tag{17}$$

But how do we actually get an estimate of c? There are several approaches. The first is to estimate the dry-rock Poisson's ratio, σ_{dry}, noting that this is given by:

$$\sigma_{dry} = \frac{\left[\frac{V_P}{V_S}\right]_{dry}^2 - 2}{2\left[\frac{V_P}{V_S}\right]_{dry}^2 - 2} = \frac{c-2}{2c-2} . \tag{18}$$

Generally, the accepted value of σ_{dry} is in the order of 0.1, which corresponds to a V_P/V_S ratio of 1.5, or a c value of 2.25.

A second approach is to perform laboratory measurements. Murphy et al (1993) measured the K_{dry}/μ ratio for clean quartz sandstones over a range of porosities and found that this value was, on average, equal to 0.9. This corresponds to a c value of 2.233. If the K_{dry}/μ value is rounded to 1.0, this implies a σ_{dry} of 0.125, and a corresponding c value of 2.333.

Thus, there are a range of values of c that depend on the particular reservoir being studied. Table 1 shows a range of c values and the range of respective elastic constants. The value of c in this table ranges from a high of 3, which implies that λ_{dry}/μ is equal to 1, to a low of 1 1/3, which implies that K_{dry}/μ is equal to 0. (This also implies that the material has infinite compressibility.) This last value may come as a shock to many readers, especially when it is noted that the values of σ_{dry} and λ_{dry}/μ are negative! However, it was suggested by Leon Thomsen (personal communication) that materials with negative Poisson's ratios do exist, so we should include this value as an end member.

$c = \left(\frac{V_P}{V_S}\right)^2_{dry}$	$\left(\frac{V_P}{V_S}\right)_{dry}$	σ_{dry}	$\frac{K_{dry}}{\mu}$	$\frac{\lambda_{dry}}{\mu}$
3.000	1.732	0.325	1.667	1.000
2.500	1.581	0.167	1.167	0.500
2.333	1.528	0.125	1.000	0.333
2.250	1.500	0.100	0.917	0.250
2.233	1.494	0.095	0.900	0.233
2.000	1.414	0.000	0.667	0.000
1.333	1.155	-1.000	0.000	-0.667

Table 1: A table of values for *c*, ranging from 3 to 1 1/3 showing the equivalent values for various elastic constant ratios.

Using the values of c given in Table 1, let's return to the three references from the introduction (those of Goodway et al (1997), Hedlin (2000), and Hilterman (2001)) and interpret their results. Goodway et al attribute all of the fluid effect to the λ term in equation (1), and thus derive their $\lambda\rho$ value as

$$\lambda\rho = Z_P^2 - 2Z_S^2 \quad . \tag{19}$$

Note that this means that c is equal to 2, and implies a dry rock Poisson's ratio of zero.

Hedlin (2000) incorporated the experimental results of Murphy et al, to arrive at the K_{dry}/μ ratio of 0.9 and a c value of 2.233. Hedlin calls this the K_P-μ method. Finally, Hilterman (2001, Figure 6.A.6) assumes that K_{dry}/μ is equal to 1.0, which implies a c value of 2.333.

So, is there a correct value for c? Let's try and answer this question by looking at numerical well-log and seismic-data examples.

NUMERICAL EXAMPLE

As a numerical example of the concepts discussed in the last section, let's examine the Class 1, 2, and 3 sand models given in Figure 4.B.2 of Hilterman (2001). These models were derived from Gulf of Mexico trend curves where the wet-sand S-wave velocities were estimated with the Greenberg-Castagna technique and the fluid properties were derived with the Batzle-Wang approach.

We have mentioned that both the P and S-wave impedances are assumed to be available for discrimination of the pore-fluid saturant. In addition, we have proposed the additional attributes of ρs and ρf for discrimination. These potential discriminators are listed in Table 2 for Class 1, 2, and 3 AVO environments. For

Class 3, which is a bright-spot environment, the difference in the P-wave acoustic impedance between a wet sand and a gas sand is significant enough to discriminate the pore fluids. However, in the Class 1 environment, the P-wave acoustic impedances for a wet sand and gas sand have similar values. Thus, differentiation of the gas-saturated sand from wet sand would be difficult with P-wave acoustic impedance. However, the ρf attribute will differentiate the two different pore saturants in all three sand models. The c values that are listed in the last column of Table 2 are highly dependent on the V_P/V_S transform. Thus, besides being in an acceptable range, conclusions based on the proper selection of the c value should be dependent on locally measured logs. This is accomplished in the well-log example given in the next section.

Class 3 AVO

	P-Wave (km/s)	S-Wave (km/s)	Density (g/cc)	AI(P)	AI(S)	ρs	ρf	c
Wet Sand	2.134	0.860	2.110	4.502	1.814	7.782	12.485	2.366
Gas Sand	1.543	0.901	1.880	2.900	1.694	6.934	1.476	2.366

Class 2 AVO

	P-Wave (km/s)	S-Wave (km/s)	Density (g/cc)	AI(P)	AI(S)	ρs	ρf	c
Wet Sand	3.048	1.595	2.230	6.797	3.557	34.150	12.050	2.699
Gas Sand	2.781	1.665	2.080	5.785	3.463	31.853	1.615	2.699

Class 1 AVO

	P-Wave (km/s)	S-Wave (km/s)	Density (g/cc)	AI(P)	AI(S)	ρs	ρf	c
Wet Sand	4.115	2.453	2.320	9.546	5.691	82.826	8.309	2.557
Gas Sand	4.050	2.526	2.210	8.951	5.583	78.899	1.221	2.557

Table 2. The gas and wet sand AVO examples from Figure 4.B.2 of Hilterman (2001) for several values of *c*.

WELL LOG EXAMPLE

Our well-log example comes from the Whiterose area of offshore eastern Canada. Figure. 2 shows the V_S, V_P, density and porosity logs over the producing zone, overlain by a Cretaceous shale. There is 85m of gas sand, 97m of oil sand, and 95m of wet sand. These well-log curves were converted to the equivalent ρf and ρs curves and crossplotted.

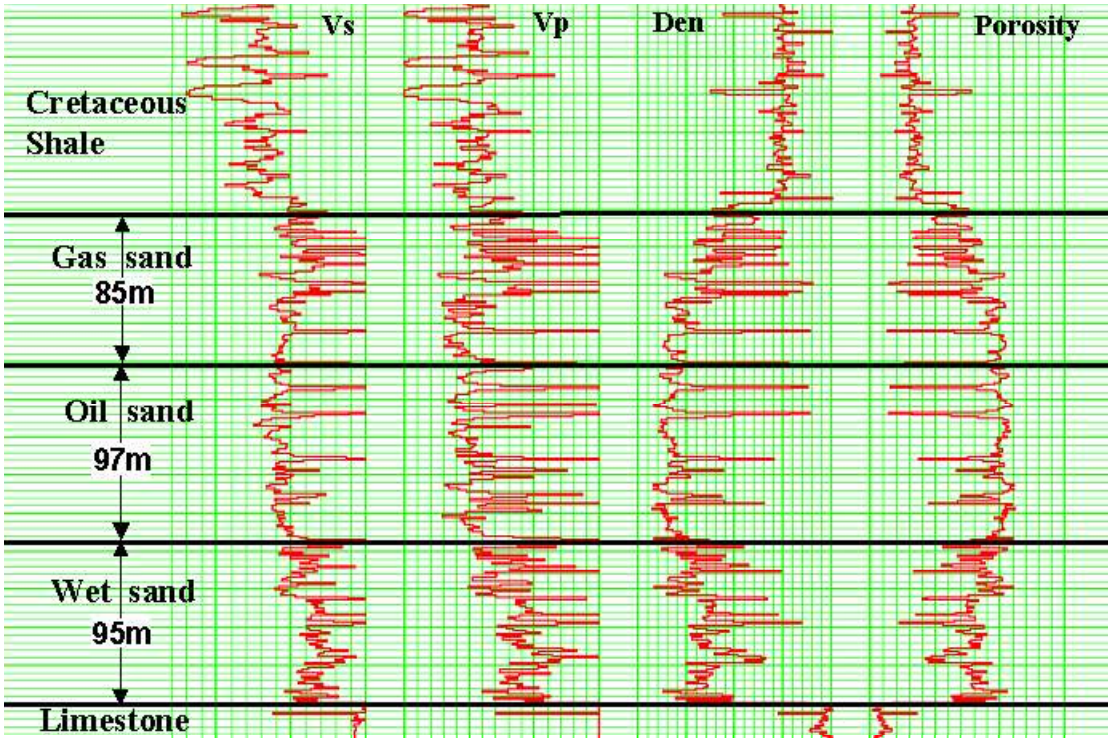

FIG. 2. The V_S, V_P, Density, and porosity logs over the producing zone in the Whiterose L-08 well.

Figure 3(a) through (d) show crossplots of the ρs versus ρf for values of c equal to 1.333, 2, 2.333, and 2.5, respectively. Each lithology and pore-fluid saturant is indicated by a different symbol. From our previous discussion, we wish to find the c value that produces the best ρf separation between the gas and non gas-saturated zones. The end members of 1.333 and 2.5 were rejected as choices for c, the former because the separation would be a sloping line, and the latter because the gas zones have negative ρf. When choosing between the other two c values, notice that the ρf separation is almost the same. However, the better choice would appear to be 2.333 since the points with a higher ρs value show better separation. Also, for the c value of 2.333, the cloud of gas points is closer to the zero value on the ρf axis. However, a value of 2.0, which corresponds to the lambda-mu-rho method of Goodway et al (1997), would also give a good separation of the gas points. Finally, we note that the crossplot for a c value equal to 2.233 (which comes from Murphy et al and Hedlin) was not shown since it produced a result that was very close to the results produced with a c value of 2.333.

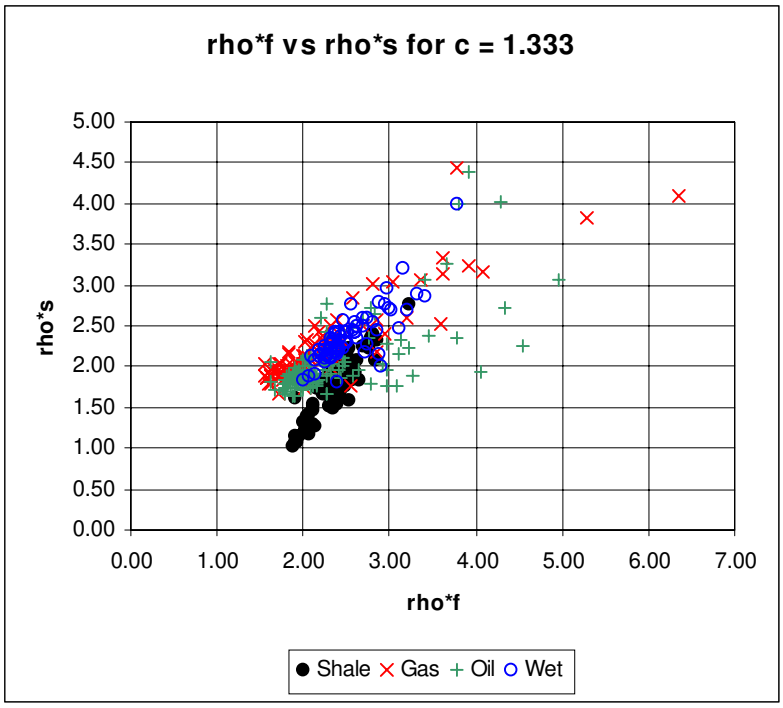

FIG. 3(a). A crossplot of ρf vs ρs for the Whiterose L-03 productive zone, where c=1.333.

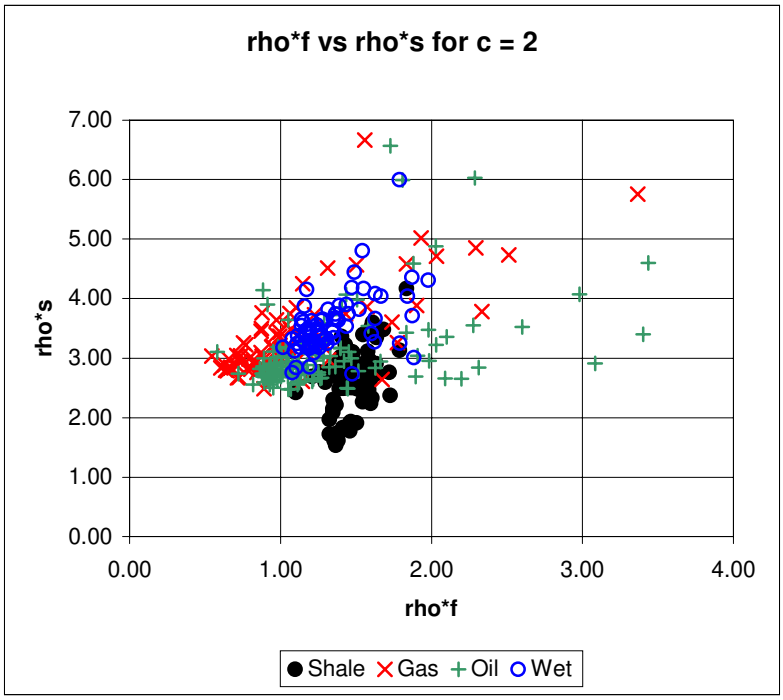

FIG. 3(b). A crossplot of ρf vs ρs for the Whiterose L-03 productive zone, where c=2.0.

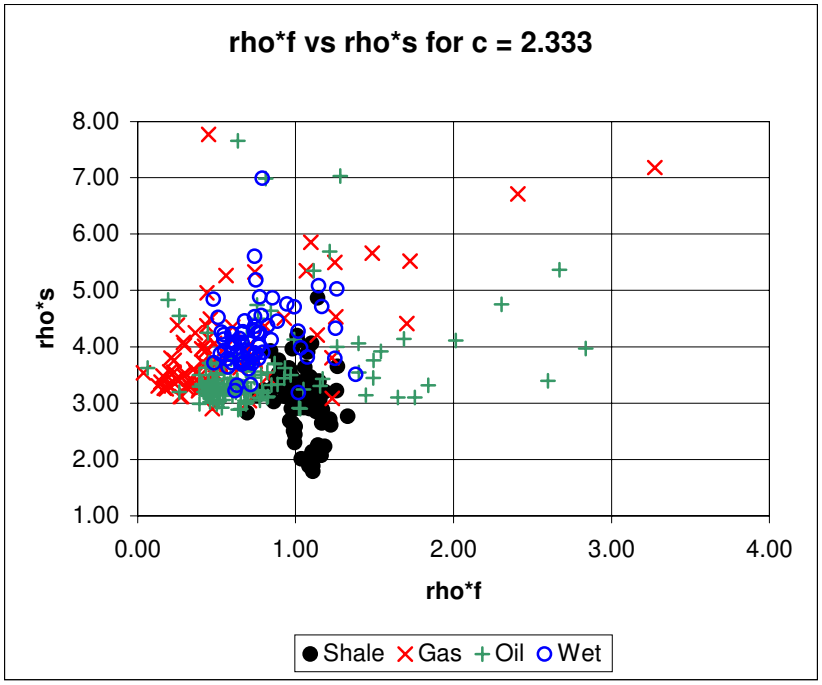

FIG. 3(c). A crossplot of ρf vs ρs for the Whiterose L-03 productive zone, where c=2.333.

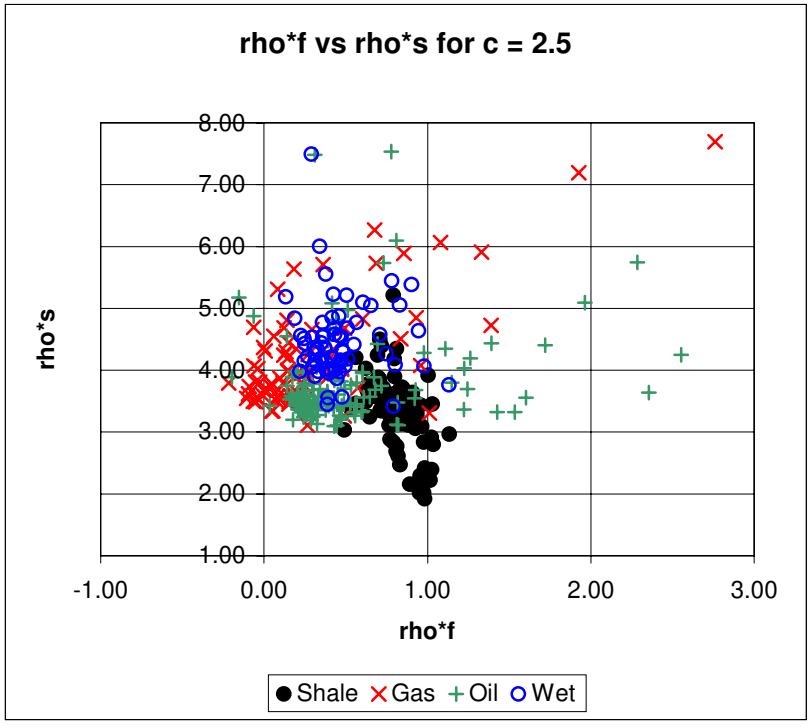

FIG 3(d). A crossplot of ρf vs ρs for the Whiterose L-03 productive zone, where c=2.5.

A SEISMIC EXAMPLE

Now that we have looked at the fundamentals of Biot-Gassmann theory, and numerical and well-log examples, let's see how we can extract the fluid term using the AVO method. Fatti et al (1994) showed how a weighted stack could be used to extract separate estimates of the zero-offset P-wave reflectivity, R_{P0}, and S-wave reflectivity, R_{S0}, from the AVO response of prestack P-wave data. Their method is very powerful because it allows one to introduce a time-varying V_P/V_S ratio that is based on a V_P/V_S transform and the measured seismic P-wave velocity function. However, it can also be shown that, if we use the first two terms of the linearized Aki-Richards equation, or

$$R(\theta) = A + B\sin^2\theta \quad , \tag{20}$$

where $R(\theta)$ is the reflection amplitude as a function of angle θ, A is the intercept, and B is the gradient, and assume that V_P/V_S is equal to 2.0, then

$$R_{P0} = A \quad , \tag{21}$$

and

$$R_{S0} = \frac{A - B}{2} \quad . \tag{22}$$

These reflectivity estimates can then be inverted using a standard inversion technique to provide estimates of P and S-wave impedance, Z_P and Z_S. Figures 4 and 5 show the P- and S-wave impedance inversions for a shallow clastic gas-sand in Alberta.

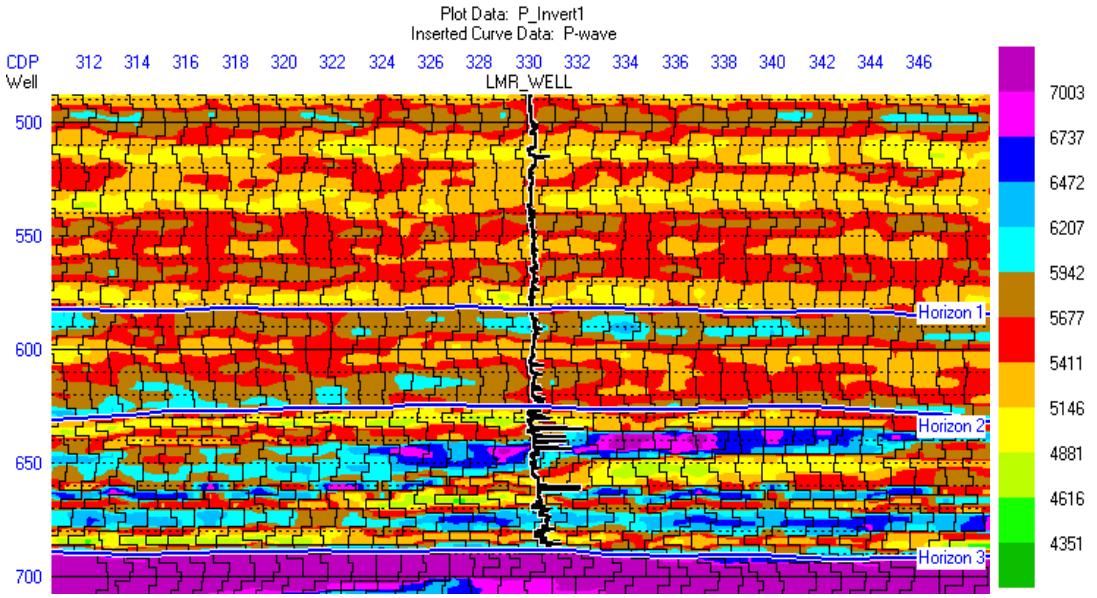

FIG. 4. The P-wave impedance, Z_P, found by inverting the R_S estimate of a shallow gas sand in Alberta.

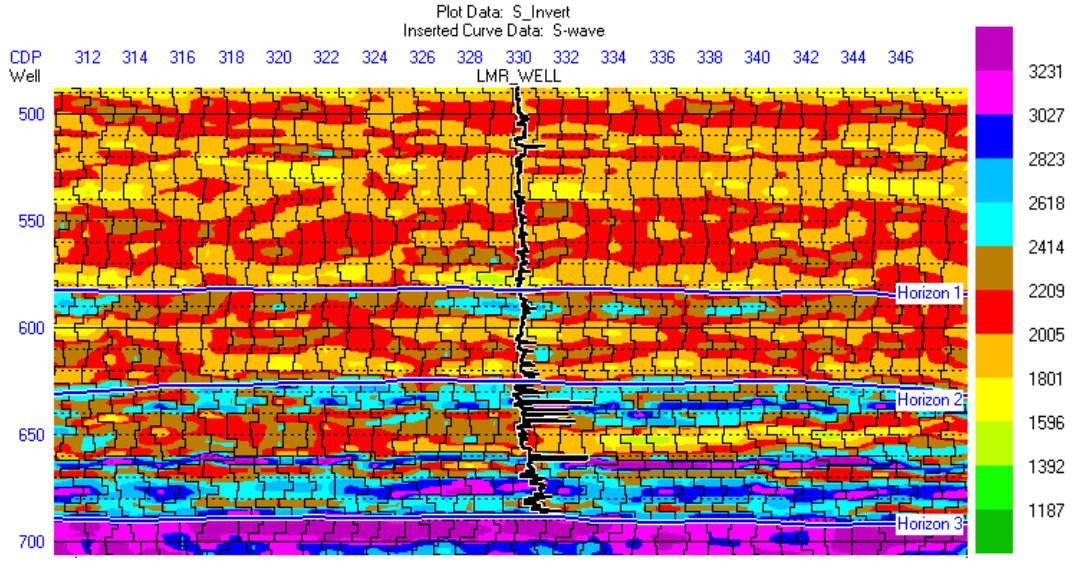

FIG. 5. The S-wave impedance, Z_S, found by inverting the R_S estimate of a shallow gas sand in Alberta.

Horizon 2 in both figures is the top of the gas sand. Notice that the P-wave impedance in Figure 4 indicates that the gas sand shows a drop in P-impedance with respect to the encasing shale. However the S-impedance in FIG. 5 does not show the same decrease as we move into the gas sand. This can be physically understood when we recall that S-wave velocity is insensitive to the fluid, whereas P-wave velocity shows a sudden decrease when gas is introduced into the reservoir. Figures 6 and 7 show the fluid and skeleton terms (ρf and ρs) computed from the P- and S-impedance sections of Figures 4 and 5, where we used a c value of 2. This means that the ρf section can be interpreted as $\lambda\rho$, whereas the ρs section can be interpreted as $\mu\rho$. Note that these sections behave exactly as we would expect. That is, the $\lambda\rho$ section of Figure 6 shows a strong decrease in the gas-filled reservoirs, whereas the $\mu\rho$ section of Figure 7 shows an increase in the reservoir (since the sand matrix has a higher value than the overlying shale).

Figure 8 shows a $\lambda\rho$ vs $\mu\rho$ crossplot between the productive zones of the two sections, with the gas sand clearly visible. Since $\mu\rho$ is plotted on the vertical axis, the separation between the gas sand and the surrounding sediments is vertical, with gas coloured red, and non-gas coloured light blue. Figure 9 then shows the corresponding zones on the seismic section plotted from the crossplot of Figure 8. The gas zone is exactly where we would expect to see it.

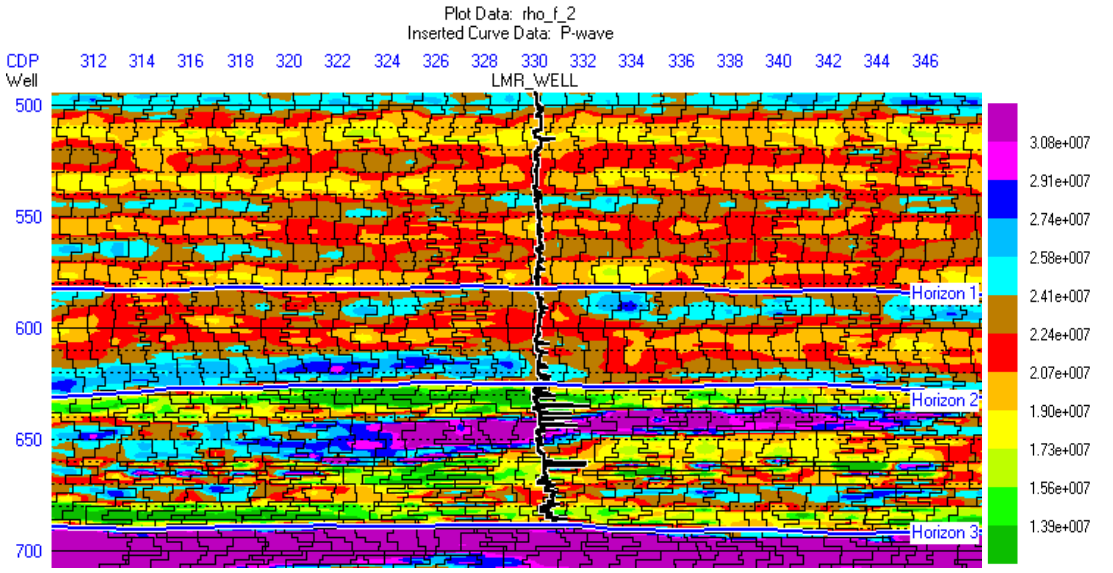

FIG. 6. The ρf section found by combining the Z_P and Z_S inversions of Figures 4 and 5 using c value of 2.

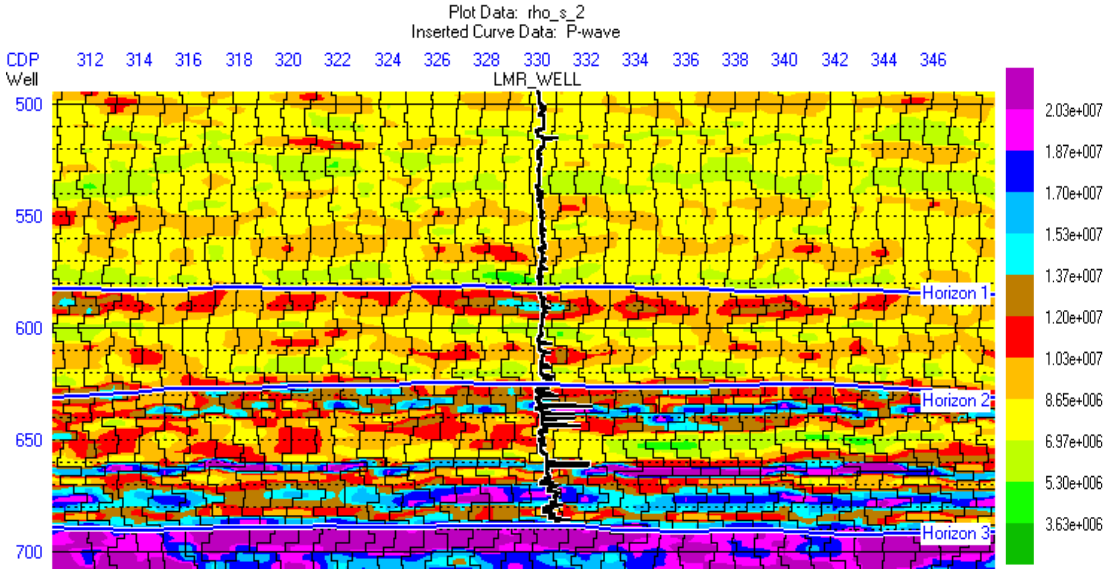

FIG. 7. The ρs section found by combining the Z_P and Z_S inversions of Figures 4 and 5 using c value of 2.

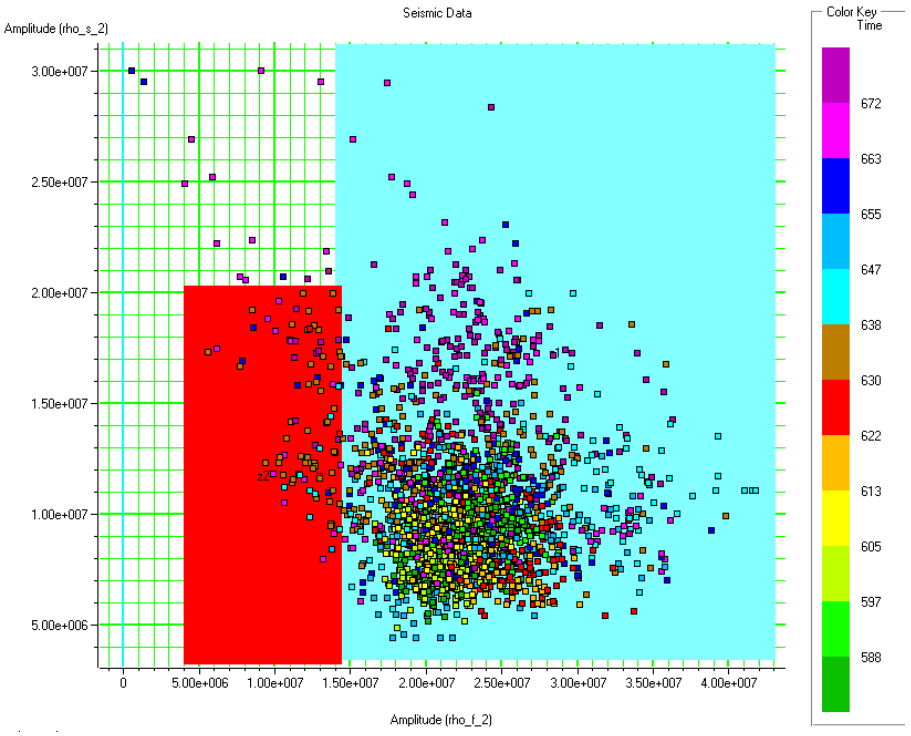

FIG. 8. A crossplot between the $\rho\phi$ and $\rho\sigma$ sections of the previous two figures, over the productive zone.

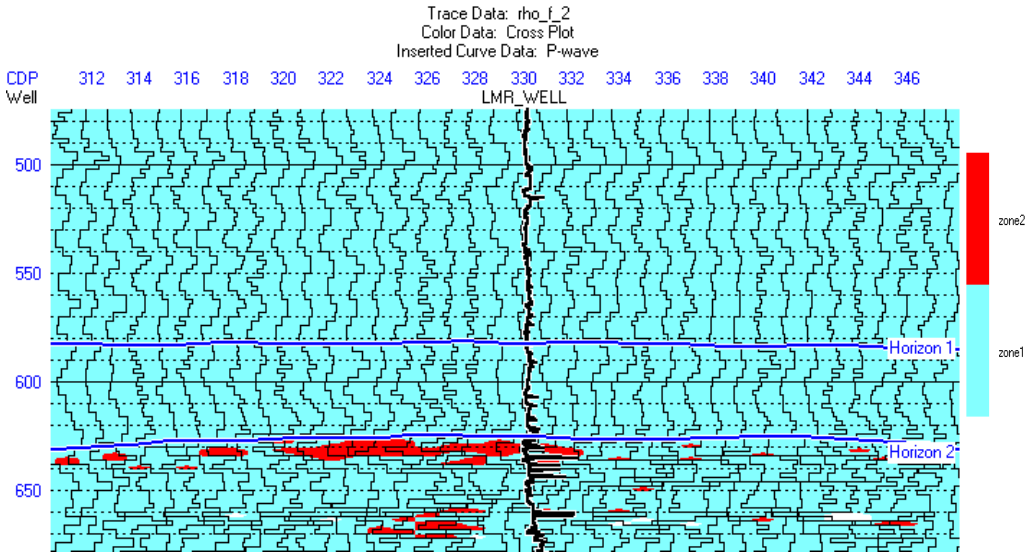

FIG. 9. The portion of the seismic section corresponding to the gas and non-gas zones. The "red" gas region is exactly where expected.

Next, we repeated the same analysis using a c value of 2.333. Figures 10 and 11 show the fluid and skeleton terms (ρf and ρs) computed from the P- and S-impedance sections of Figures 5 and 6, with this new constant. Note that these sections are very similar to those computed using a value of 2.0, (Figures 6 and 7) but show some slight differences at the pay zone.

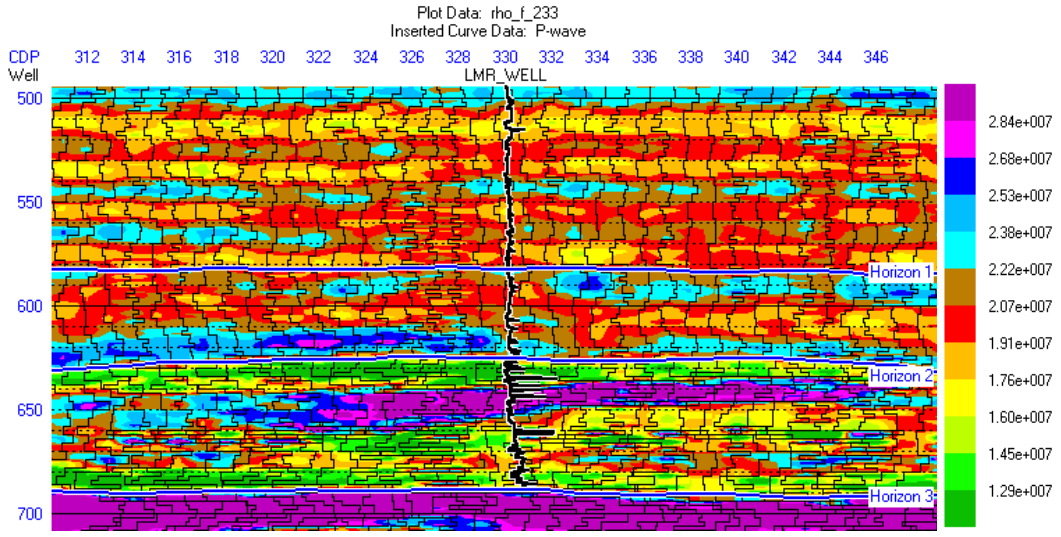

FIG. 10. The ρf section found by combining the Z_P and Z_S inversions of Figures 4 and 5 using c value of 2.333.

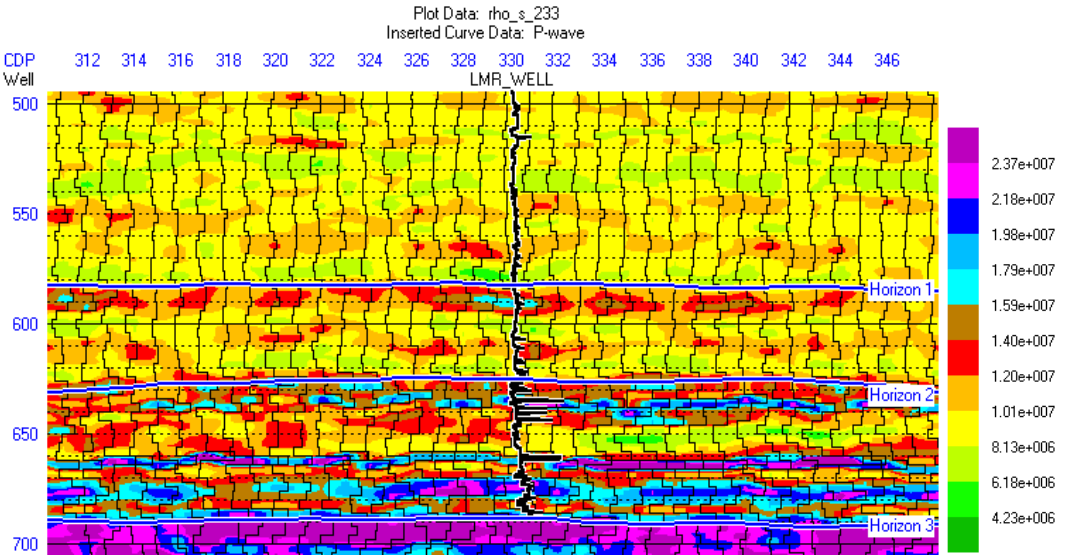

FIG. 11. The ρs section found by combining the Z_P and Z_S inversions of Figures 4 and 5 using c value of 2.333.

Figure 12 shows the crossplot between the productive zones for the two sections of Figures 10 and 11, where the gas sand is again clearly visible. Figure 13 then shows the corresponding zones on the seismic section plotted from the crossplot of Figure 11. Note that, although the change is slight, there is improved continuity at the gas sand level. Thus, although the value of 2.333 would appear to be a better value to use based on well-log data, it is only marginally better on our real data example. We would recommend determining the optimum value for c using well-log data, where possible.

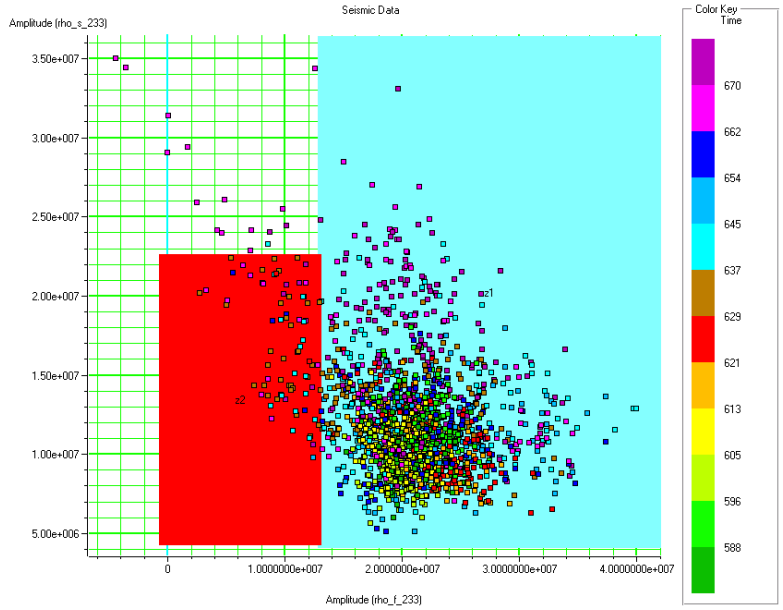

FIG. 12. A crossplot between the $\rho\phi$ and $\rho\sigma$ sections of the previous two figures, over the productive zone.

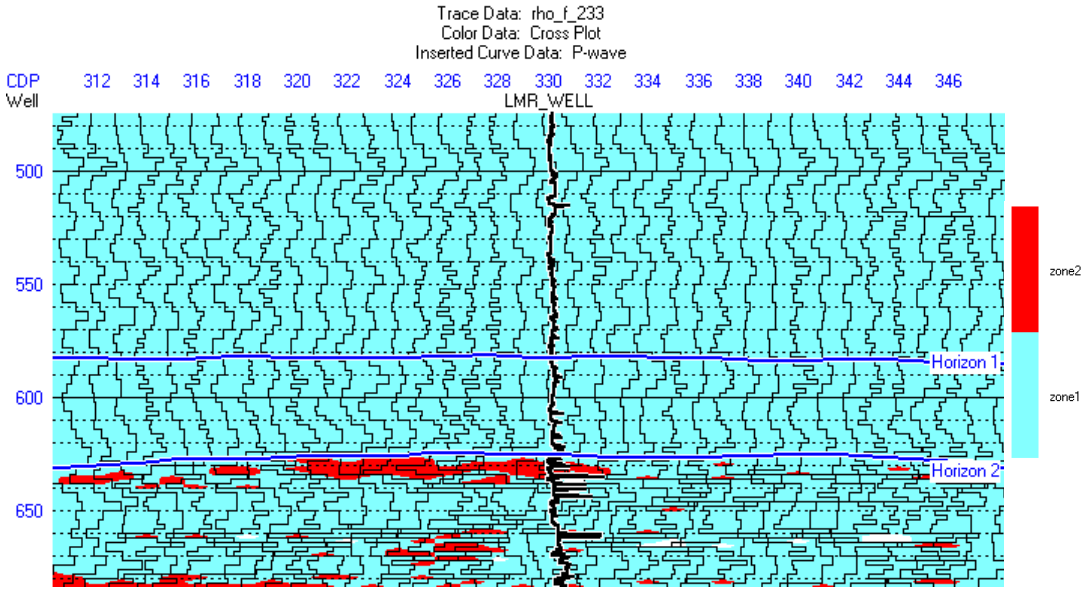

FIG. 13. The portion of the seismic section corresponding to the gas and non-gas zones. The "red" gas region is exactly where expected.

CONCLUSIONS

In this paper, we have discussed Biot and Gassmann's theory and shown how this theory can be applied to the extraction of information about the fluid properties of the reservoir. We have also shown how the lambda-mu-rho technique, the pore modulus method, and the fluid discriminant are all related through the constant value used in a weighted difference stack between P-impedance squared and S-impedance squared. Our well-log example indicated that the value of this constant should be in the order

of 2.333, whereas our real data was less conclusive and indicated that a value of 2.0 was acceptable. It would seem advisable to determine this value from well log data where it is available. These initial tests on the ρf attribute are encouraging in that it has proven to be a more sensitive discriminator of pore-fluid content than conventional inversions. The sensitivity results are consistent from the numerical models and actual well-log examples through to the testing on real seismic data.

ACKNOWLEDGEMENTS

We would like to thank Dan Hampson, Larry Mewhort, Leon Thomsen, and Jon Downton for their input to this tutorial.

REFERENCES

Batzle, M., and Wang, Z., 1992, Seismic properties of fluids: Geophysics, **57**, 1396-1408.

Biot, M.A., 1941, *General theory of three-dimensional consolidation*, Journal of Applied Physics, **12**, 155-164.

Castagna, J.P., Batzle, M.L., and Eastwood, R.L., 1985, *Relationships between compressional-wave and shear-wave velocities in clastic silicate rocks*, Geophysics, **50**, 571-581.

Domenico, S. N., 1974, *Effect of water saturation on seismic reflectivity of sand reservoirs encased in shale*, Geophysics, **39**, 759-769.

Fatti, J., Smith, G., Vail, P., Strauss, P., and Levitt, P., 1994, *Detection of gas in sandstone reservoirs using AVO analysis: a 3D Seismic Case History Using the Geostack Technique*, Geophysics, **59**, 1362-1376.

Gassmann, F., 1951, *Uber die Elastizitat poroser Medien*, Vierteljahrsschrift der Naturforschenden Gesellschaft in Zurich, **96**, 1-23.

Goodway, W., Chen, T., and Downton, J., 1997, *Improved AVO fluid Detection and Lithology Discrimination Using Lame Petrophysical Parameters*, Extended Abstracts, Soc. Expl. Geophys., 67th Annual International Meeting, Denver.

Greenberg, M.L. and Castagna, J.P., 1992, Shear-wave estimation in porous rocks: Theoretical formulation, preliminary verification and applications: Geophys. Prosp., **40**, 195-210.

Hedlin, K., 2000, *Pore Space Modulus and Extraction using AVO*, Extended Abstracts, Soc. Expl. Geophys., 70th Annual Meeting, Calgary.

Hilterman, F.J., 2001, *Seismic Amplitude Interpretation, 2001 Distinguished Instructor Short Course*, Distinguished Instructor Series, No. 4, Soc. Expl. Geophys.

Krief, M., Garat, J., Stellingwerff, J., and Ventre, J., 1990, *A petrophysical interpretation using the velocities of P and S waves*, The Log Analyst, Nov-Dec, 355-369.

Mavko, G., Mukerji, T., and Dvorkin, J., 1998, *The rock physics handbook – Tools for seismic analysis in porous media*, Cambridge University Press.

Murphy, W., Reischer, A., and Hsu, K., 1993, *Modulus Decomposition of Compressional and Shear Velocities in Sand Bodies*, Geophysics, **58**, 227-239.

Wyllie, M.R.J., Gregory, A.R., and Gardner, L.W., 1956*, Elastic wave velocities in heterogeneous and porous media,* Geophysics, **21**, 41-70.